Title
Protein Primary Structure of the Vaccinia Virion at Increased Resolution

Journal
Journal of Virology, 90(21)

ISSN
0022-538X

Authors
Ngo, Tuan
Mirzakhanyan, Yeva
Moussatche, Nissin
et al.

Publication Date
2016-11-01

DOI
10.1128/jvi.01042-16

Peer reviewed

AMERICAN SOCIETY FOR MICROBIOLOGY | Journal of Virology

Protein Primary Structure of the Vaccinia Virion at Increased Resolution

Tuan Ngo,[a] Yeva Mirzakhanyan,[a] Nissin Moussatche,[b] Paul David Gershon[a]

Department of Molecular Biology & Biochemistry, University of California—Irvine, Irvine, California, USA[a]; University of Florida, Gainesville, Florida, USA[b]

ABSTRACT

Here we examine the protein covalent structure of the vaccinia virus virion. Within two virion preparations, >88% of the theoretical vaccinia virus-encoded proteome was detected with high confidence, including the first detection of products from 27 open reading frames (ORFs) previously designated "predicted," "uncharacterized," "inferred," or "hypothetical" polypeptides containing as few as 39 amino acids (aa) and six proteins whose detection required nontryptic proteolysis. We also detected the expression of four short ORFs, each of which was located within an ORF ("ORF-within-ORF"), including one not previously recognized or known to be expressed. Using quantitative mass spectrometry (MS), between 58 and 74 proteins were determined to be packaged. A total of 63 host proteins were also identified as candidates for packaging. Evidence is provided that some portion of virion proteins are "nicked" via a combination of endoproteolysis and concerted exoproteolysis in a manner, and at sites, independent of virus origin or laboratory procedures. The size of the characterized virion phosphoproteome was doubled from 189 (J. Matson, W. Chou, T. Ngo, and P. D. Gershon, Virology 452-453:310–323, 2014, doi:http://dx.doi.org/10.1016/j.virol.2014.01.012) to 396 confident, unique phosphorylation sites, 268 of which were within the packaged proteome. This included the unambiguous identification of phosphorylation "hot spots" within virion proteins. Using isotopically enriched ATP, 23 sites of intravirion kinase phosphorylation were detected within nine virion proteins, all at sites already partially occupied within the virion preparations. The clear phosphorylation of proteins RAP94 and RP19 was consistent with the roles of these proteins in intravirion early gene transcription. In a blind search for protein modifications, cysteine glutathionylation and O-linked glycosylation featured prominently. We provide evidence for the phosphoglycosylation of vaccinia virus proteins.

IMPORTANCE

Poxviruses are among the most complex and irregular virions, about whose internal structure little is known. To better understand poxvirus virion structure, imaging should be supplemented with other tools. Here, we provide a deep study of the covalent structure of the vaccinia virus virion using the various tools of contemporary mass spectrometry.

Contemporary mass spectrometry (MS) instrumentation provides an avenue for proteome coverage with enormous breadth or depth, depending upon the complexity of the proteome. Typically, the power of the approach is exploited for breadth in the analysis of increasingly complex proteomes. Here, we have taken a relatively narrow proteome, that of a virus particle, and explored proteome depth, developing analytical approaches and tools as required.

Sporadic information is available on the covalent (primary) molecular structure of the vaccinia virus virion. Around 75 proteins can be detected in two-dimensional (2D) gels of purified vaccinia virus virions (1). Three published MS studies provided early compendia of viral and host gene products present within vaccinia virus and human monkeypox virion preparations via MS (2–5). These studies built upon earlier, less comprehensive studies that employed a combination of MS and N-terminal sequencing (1, 6). Overlapping approaches in terms of instrumentation, preparation, and data analysis led to an overlapping set of detected gene products.

In terms of covalent protein modifications, six vaccinia virus proteins can be labeled *in vivo* with myristate, five of which have been identified as L1R (7, 8), G9R, A16L, and E7R (9), and A14L (10). All except A14L possess a glycine at position 2 in the protein. At least eight vaccinia virus-encoded proteins may be palmitoylated, as evidenced by the incorporation of ^{3}H-labeled palmitate in culture (11). These proteins include wrapped virus (WV)-specific protein p37 (F13L) (7, 12–14) and products of open reading frames (ORFs) A33R (15), B5R (16), F13L (17), the A22R Holliday resolvase (11), A36R, and the A56R hemagglutinin (11).

Glycosylation has been clearly detected among the wrapping membrane proteins of wrapped vaccinia virus (WV): A33L protein was identified as a glycoprotein based on the mobility of diffuse bands by sodium dodecyl sulfate-polyacrylamide gel electrophoresis (SDS-PAGE) and the presence of NX(S/T) sites in the extracellular domain (15). Examination of A33L protein produced in the presence of tunicamycin or monensin (14), inhibitors of N-linked and O-linked glycosylation, respectively, indicated the possession of both N- and O-linked glycans by A33L. Use of both drugs in combination led to a discrete protein band with the predicted molecular mass of 33 kDa. Envelope protein

Received 27 May 2016 **Accepted** 17 August 2016

Accepted manuscript posted online 24 August 2016

Citation Ngo T, Mirzakhanyan Y, Moussatche N, Gershon PD. 2016. Protein primary structure of the vaccinia virion at increased resolution. J Virol 90:9905–9919. doi:10.1128/JVI.01042-16.

Editor: G. McFadden, University of Florida

Address correspondence to Paul David Gershon, pgershon@uci.edu.

Supplemental material for this article may be found at http://dx.doi.org/10.1128/JVI.01042-16.

A34 was identified as a glycoprotein on the basis of tunicamycin treatment leading to a discrete faster moving band (18). For protein B5R, metabolic labeling with [^{3}H]glucosamine revealed the glycosylation of this protein (16), alongside the inhibition of B5R protein production with tunicamycin (19).

WV protein modifications have also been demonstrated using monoclonal antibodies (MAbs) raised against WV (14), via the immunoprecipitation of WV surface proteins from extracts of infected cells incubated with [^{3}H]glucosamine. Again, glycosylation was confirmed using tunicamycin and monensin. Via *in vivo* labeling with [^{35}S]sulfate, the sulfation of an 89-kDa vaccinia virus glycoprotein was observed (14). An earlier, in-depth study focused on glycosylation of the vaccinia virus hemagglutinin (A56R) protein via labeling with [^{3}H]glucosamine or [^{3}H]fucose followed by lectin purification, in addition to the application of tunicamycin, alkaline hydrolysis of glycans, and use of glycosidases (20). Via these combined approaches, both N-linked and O-linked glycosylation of A56R protein were reported. It has been suggested that none of the MV membrane proteins are glycosylated, with important implications for the derivation of the viral membrane (21).

Recently, the vaccinia virus virion phosphoproteome was reported (22), revealing the confident identification of 189 sites of phosphorylation within virus proteins.

During virion maturation, several vaccinia virus proteins are subject to processing in the form of one or two proteolytic cleavages (23). These proteins include the products of genes A10L (p4a), A3L (p4b), G7L, A12L, L4R, and A17L. Proteolysis occurs C terminal to the Ala-Gly sequence (24–26).

Here, we have explored the covalent structure of the vaccinia virus virion. We took a longitudinal approach to protein MS analysis, leading to a comparatively rich survey of the virion proteome. We demonstrate the detection of 88% known vaccinia virus ORFs in just purified virion preparations alone, including the first detection of products from 27 ORFs previously designated "predicted," "uncharacterized," "inferred," or "hypothetical." Using quantitative MS, we show the packaging of 58 to 74 ORF products in the virion. Evidence is provided that a portion of virion proteins are "nicked" via a combination of endoproteolysis and concerted exoproteolysis. The size of the characterized virion phosphoproteome was increased from 189 (22) to 396 confident, unique phosphorylation sites, of which 268 were within the packaged protein set. Using isotopically enriched ATP, 23 sites of intravirion kinase phosphorylation were confidently detected within nine virion proteins. Finally, in a blind search for protein modifications, cysteine glutathionylation and N-linked and (in particular) O-linked glycosylation featured prominently. We also provide evidence for the phosphoglycosylation of vaccinia virus proteins.

MATERIALS AND METHODS

Virus. Sucrose-purified vaccinia virus WR, originally from the Moss laboratory, has been described (22). Tartrate-purified vaccinia virus WR, originally from the Condit lab (with a BamHI cleavage site in the I3L gene), was prepared as described previously (27). ATP (γ-P^{18}O$_4$, 97%), referred to here as ^{18}O-ATP was from Cambridge Isotope Laboratories Inc.

Virion proteome. Virus protein was assayed by bicinchonic acid, according to the manufacturer's recommendations (ThermoFisher, Inc.). Aliquots of virus representing 15 to 60 μg of total protein were pelleted from storage buffer, and pellets were dissolved in 36 mM sodium lauroylsarcosine, 36 mM sodium deoxycholate, 5 mM tris(2-carboxyethyl)phosphine (TCEP), and 50 mM triethylammonium bicarbonate (TEAB). Virus was dissolved by repeated heating/ultrasonication and then diluted 15-fold with 50 mM TEAB and 5 mM TCEP, followed by the addition of trypsin at an enzyme/substrate mass ratio of 1:100. After overnight incubation at 37°C, followed by the addition of a second equivalent aliquot of trypsin and further incubation for 2 to 4 h, an equal volume of ethyl acetate was added, along with trifluoroacetic acid (TFA) to a final concentration of 65 mM. The solvent-extracted aqueous phase was applied to a stacked C_{18}-SCX (strong cation exchange) StageTip, and peptides transluted to the SCX phase with 80% CN_3CN–0.1% formic acid (FA), followed by sequential elution with 160, 200, 255, 325, 540, and 800 mM ammonium acetate in 20% CH_3CN–0.5% FA, followed by 5% NH_4OH in 80% CH_3CN (40 μl/10 μg protein loaded). Each elution was evaporated to dryness and then redissolved in 12 μl of 0.1% FA in water for nanocapillary liquid chromatography coupled with tandem mass spectrometry (nanoLC-MS/MS).

For comparison of GluC, Arg, and AspN with trypsin, virion protein mixture (VPM) was generated by dissolving virus pellet in 8 M urea and 50 mM ammonium bicarbonate, incubating with 5 mM TCEP for 30 min at 37°C, and then incubating with 5 mM iodoacetamide for 30 min in the dark. For AspN digestion (and the trypsin control digestion), VPM was diluted 8-fold with 50 mM NH_4HCO_3 (pH 8.0) and AspN (Roche Diagnostics), or trypsin was added at an enzyme/substrate mass ratio of 1:100, followed by overnight incubation at 37°C. For GluC digestion, VPM was diluted 16-fold with 50 mM NH_4HCO_3 (pH 8.0), and GluC (Promega) was added and incubated as described above. For ArgC digestion, VPM was diluted 8-fold with 50 mM NH_4HCO_3 (pH 7.6) and then TCEP was added to a final concentration of 4 mM followed by ArgC (Promega) at an enzyme/substrate mass ratio of 1:100 and digested overnight at 37°C. Samples were acidified with 100% FA to pH between 1 and 3 and then desalted with a stacked StageTip as described above, except that transluted samples were eluted from the SCX phase directly with a single step of 5% NH_4OH in 80% CH_3CN, then evaporated to dryness, and redissolved in 12 μl of 0.1% FA in water for nanoLC-MS/MS.

For CNBr or CNBr-trypsin cleavage, pelleted virus was suspended directly in 70% FA, and a crystal of fresh CNBr was added, followed by incubation at room temperature overnight and then drying in a vacuum. Samples were then either redissolved in 0.1% FA or redissolved in 50 mM TEAB and 5 mM TCEP followed by trypsin addition at an enzyme/substrate mass ratio of 1:100, overnight incubation, and acidification with 100% FA to pH between 1 and 3. Samples were then applied to a stacked StageTip as described above and then desalted by using a StageTip as for nontrypsin enzymes. For quantitative MS, peptide dimethyl isotope labeling was performed as described previously (28).

For nanoLC-MS/MS, 2-μl aliquots were injected with a tip (75 μm by 25 cm) that was made in-house and packed with C_{18} beads (MacMod), using a nanoLC-Easy 1000 instrument, followed by a segmented linear gradient of 0 to 35% CH_3CN–0.1% FA in 0.1% FA–water over 240 min at 0.25 μl/min. Spectra were acquired using an Orbitrap Velos Pro instrument (ThermoFisher). Each precursor ion spectrum (Fourier transform mass spectrometry [FTMS], 60,000 resolution, 380 to 2,000 Thomson [Th]) was followed by up to 20 MS2 spectra of the most abundant precursor ions with a signal of >1,000 and 2+ or higher charge, in ion trap rapid CID (collision-induced dissociation) mode, with dynamic exclusion. For CNBr-trypsin-cleaved samples, HCD (higher-energy collisional dissociation) fragmentation was used in place of ion trap rapid CID, and for samples cleaved with CNBr alone, rapid CID was replaced with either HCD or ETD (electron transfer dissociation) fragmentation. All ETD spectra employed an activation time of 0.1 s, plus or minus supplemental activation. For HCD, the most abundant ions with a signal of >5,000 and 2+ or higher charge in each precursor spectrum (up to a total of 15 ions) were fragmented, and MS2 spectra were acquired in Fourier transform mode with 7,500 resolution, normalized collision energy of 30%, and an activation time of 0.1 ms. For dimethyl-labeled samples, data were acquired in profile mode; for all other samples, centroid data acquisition was used.

Raw spectra were subjected to Mascot Distiller peak processing (Mascot Distiller 2.5.0.0), followed by MS/MS ion searches of monoisotopic experimental masses using the Mascot 2.5.0 or 2.5.1 search engine. The Mascot database for DNA-level searches was generated from the vaccinia virus reference genome (WR strain [GenBank accession no. NC_006998]). Protein-level searches employed, as the database, Swiss-Prot 2014_07 or Swiss-Prot 2015_02 with included taxonomies of human and vaccinia virus WR (Taxonomy IDs of 9606 and 10254, respectively), along with a database of common contaminants. Some protein-level searches also included a database of protein sequences generated from the GenBank annotation of NC_006998. All searches included a decoy database. For CID data sets, precursor and fragment mass tolerances were ±30 ppm and ±0.5 Da, respectively, and for HCD data sets, they were ± 20 ppm and ± 20 millimass units, respectively. Searches allowed up to one missed cleavage and no fixed modifications. For all searches except CNBr or CNBr-trypsin searches, variable modifications were as follows: deamidated (NQ), dioxidation (C), oxidation (C), and oxidation (M). For CNBr-cleaved samples, variable modifications included Met→L-homoserine and Met→L-homoserine lactone and lacked oxidation (C). For CNBr-trypsin-cleaved samples, Gln→pyro-Glu and Glu→pyro-Glu were also included as variable modifications. The instrument type selected for ETD data was "ETD-TRAP," and for all other searches, it was "ESI-TRAP." Cleavage specificity (trypsin, semitrypsin, GluC, ArgC, AspN, CNBr, and CNBr plus trypsin) reflected the reagents used. Mascot search exports retained the calculated false-discovery rate (FDR) for the initial significance threshold if <5%, otherwise results were manually recalculated with a FDR threshold of 5% and/or 1%. GenBank entry M35027.1 was used for the Copenhagen strain genome sequence. Dimethyl-labeled samples were quantitated using Mascot Distiller 2.5.1 as described previously (28).

Blind modification search. Results from Mascot searches, as described above, were reported with a FDR threshold of 1%, and the significance threshold was recorded. Subsequent "error-tolerant" Mascot searches, for which decoy searches are not available, were performed with a FDR threshold of "pseudo-1%" using this significance threshold value.

^{18}O phosphorylation. Aliquots of virus representing 150 to 200 μg of total protein were pelleted from storage buffer and then resuspended in 10 μl of 50 mM 4-(2-hydroxyethyl)-1-piperazineethanesulfonic acid (HEPES) (pH 7.0 or 8.5), followed by the addition of 10 μl of 2× uncoating buffer (0.1 M HEPES [pH 7.0 or 8.5], 0.1% NP-40, 80 mM TCEP) for 5 min at room temperature with periodic vortexing/ultrasonication. After the addition of 20 μl of 2× phosphorylation buffer (0.1 M HEPES [pH 7.0 or 8.5], 80 mM TCEP, 2 mM $MgCl_2$, 2 mM ^{18}O-ATP, 2 mM spermidine, 20 mM KCl) and 1 μl of 1% NP-40, the suspension was incubated for 15 min at 37°C with periodic vortexing. Samples were then supplemented with phosphatase inhibitors (EZblock; BioVision) and 40 μl of 2× dissociation buffer (described above) followed by cycles of heating and ultrasonication. Trypsinization was performed as described above, followed by desalting using a C_{18} StageTip, eluting peptides with 80% CH_3CN–0.5% FA followed by vacuum desiccation. Phosphopeptides were isolated using either TiO_2 or immobilized metal affinity chromatography (IMAC).

(i) TiO_2. A gel loading tip with C_8 membrane frit was filled with 1 mg of TiO_2 beads (GL Sciences) in 80% CH_3CN and 5% TFA, which was then washed with 0.1 ml of 80% CH_3CN and 1% TFA (wash solution) and then with 0.1 ml of binding solution. Dried peptides were redissolved in 0.1 ml of 1 M glycolic acid, 80% CH_3CN, 5% TFA (binding solution) and then loaded onto the tip, which was then washed sequentially with 0.1 ml binding solution and 0.1 ml wash solution. For some experiments, glycolate was replaced with 1 M lactic acid. Phosphopeptides were eluted sequentially with 30 μl of 5% ammonium hydroxide, 5% piperidine, and 5% pyrrolidine, with each elution put into a separate microtube containing 30 μl of 20% TFA, after which the elutions were pooled and desalted using a C_{18} StageTip.

(ii) IMAC. Eighty microliters of PHOS-Select Iron Affinity Gel slurry (Sigma-Aldrich) was washed three times with 0.5 ml of 0.25 M acetic acid in 30% CH_3CN (pH 2.5 to 3.0) (iBinding solution), and then dried peptides were redissolved in 0.1 ml of iBinding solution and added to the gel. After incubation at room temperature for 60 min with agitation, the gel was washed with 0.5 ml of iBinding solution and then washed with 0.5 ml water. Phosphopeptides were eluted with 0.5 ml of 0.4 M ammonium hydroxide in 30% CH_3CN and then with 0.5 ml of 0.2 M sodium phosphate (pH 8.4). The pool of elutions was desalted using a C_{18} StageTip.

nanoLC-MS/MS for enriched phosphopeptide samples was performed as described above except that up to 10 of the most abundant precursor ions with a signal of >500 in each precursor spectrum were subjected to tandem fragmentation cycles via CID (as described above) and ETD with an activation time of 0.1 s and supplemental activation. Mascot searches for enriched phosphopeptide samples were conducted as described above except that the variable modifications indicated above were supplemented with the following: phospho (ST), phospho (Y), phospho-18O (ST) and phospho-18O (Y). Also, the precursor mass tolerance was ±20 ppm, and the "instrument type" was set to "CID+ETD." Significance thresholds in search results were set to allow export of all hits better than a target FDR of 5%.

All data were analyzed and reformulated using code written in-house.

RESULTS

Proteome of the vaccinia virus virion preparation. The protein content of the vaccinia virus virion has been investigated in three published MS studies (2–4) and in our previous work (22). Comparison of the above proteomes (22) indicated a set of 53 vaccinia virus proteins universally found in the virion and 112 vaccinia virus proteins not found in any of the four virion preparations. The 53-protein set may be supplemented with proteins reported to be virion (or virion core) associated via non-MS approaches, such as G5R (FEN-like nuclease [29]), G6R (core surface/lateral body protein [30]), and O3L (a very small ORF and member of the vaccinia virus entry-fusion complex [31]).

Here, we initially conducted a deep survey of the proteomes of two virion preparations, "sucrose" and "tartrate," using current instrumentation and methods. Infection, cell lysis, and virion purification conditions for the two preparations are given in Table 1. Between 147 and 173 vaccinia virus-encoded proteins from the respective preparations were identified (Table 2) from a theoretical vaccinia virus proteome based on the 211 unique VACWR-numbered ORFs in the WR reference genome (see Table S1 in the supplemental material). G5R and G6R (discussed above) were among the detected proteins. Figure 1 provides a visual impression of the progressive saturation of the viral proteome with successive analyses of virion preparations over the prior decade (based on Table S1). For example, the two leftmost orange columns were a repeat of the virus analysis shown in the (older) green column using the same virus preparation and the same MS sample preparation method, but newer instrumentation. Figure 1 illustrates the following. (i) As MS instrumentation performance evolves, the viral proteome progressively saturates. (ii) The proteome of the virion preparation must be distinct from the proteome of the virion itself. Emphasizing the latter point, greater numbers of host proteins than vaccinia virus proteins were found in the two virion preparations by a factor of between 8.5 and 22 (Table 2).

The above survey employed tryptic peptides only. The tartrate-purified virus was also digested with three alternative proteases, namely, ArgC, AspN, or GluC, or cleaved with CNBr or CNBr-trypsin (see Table S2 in the supplemental material). Although these alternative reagents did not contribute much additional coverage to the existing tryptic proteome, they provided the first ev-

TABLE 1 Infection, cell lysis, and virion purification conditions for the virion preparations used in this study[a]

Procedure(s) and characteristic	Value for characteristic	
Infection		
Host cells	HeLa suspension	BSC40 cells (adherent)
Infection cell density	2×10^7 cells/ml	2.5×10^7 cells/dish, 20 to 25 ml medium
Vaccinia virus strain	WR	WR
Infection MOI	8	0.5
Infection time (min)	30	60
Infected-cell maintenance		
Suspension density	5×10^8 cells/liter	
Type of culture	Suspension	Adherent
Medium	MEM spinner	DMEM
Serum	5% horse serum	10% FBS
Atmosphere	5% CO_2	5% CO_2
Duration of infection	2 to 3 days	4 days
Cell lysis and virus purification		
Virion preparation	Sucrose	Tartrate
Cell lysis method	Swell in 10T9, Dounce homogenize	Freeze/thaw, sonicate, Dounce homogenize in 3 ml 10T8
Nuclear spin	900 rpm, 5 min	3,000 rpm (1,200 × *g*), 10 min
Initial pellet purification method (cushion)	Through 36% sucrose in 10T9; SW27, 13.5 krpm rpm, 80 min	Through 36% sucrose SW28, 18 krpm, 80 min
Gradient purification method	5 to 40% sucrose in 1T9, continuous (2x) SW27, 12 krpm, 50 min	25 to 40% K^+ tartrate, step (1x) SW28, 25 krpm, 90 min
Pellet virus from harvested band	Dilute 1:3 with 1T9. Pellet at 13,500 rpm, 60 min.	Dilute to 34 ml/band with 10T8→SW28, 20 krpm, 30 min
Additional washes		2x as described above
Resuspend in storage buffer	1T9	10T8
Yield		466.4 OD_{260} units in 5 ml; 5.6×10^{12} particles; 5,300 particles/cell

[a] The conditions used for the infection, cell lysis, and virion purification procedures for the sucrose and tartrate virion preparations are given. K^+ tartrate was buffered with 20 mM KPO_4, pH 8.0. Abbreviations: 10T8, 10 mM Tris-HCl at pH 8.0; 10T9, 10 mM Tris-HCl at pH 9.0; 1T9, 1 mM Tris-HCl at pH 9.0; MOI, multiplicity of infection; MEM, minimal essential medium; DMEM, Dulbecco modified Eagle medium; FBS, fetal bovine serum; krpm, kilo rpm (1,000 rpm); 2x, twice; 1x, once; OD_{260}, optical density at 260 nm.

idence of expression, among the virion MS studies described above, for five additional proteins, namely, F14R, C11R (vaccinia virus growth factor [VGF]), B25R, A53R, and F6L (Table 3 and Table S1). The detection of F14R may have been favored by AspN due to its very high content of acidic residues (nearly 29%) (Table 3), with only two basic residues available for recognition by trypsin. The confident identification, via AspN and GluC, of I2L, a 73-amino-acid (aa) late protein with an apparent role in host cell entry (32) (Table 3), supported its weaker (5% FDR only) identifications with trypsin (Table S1) and its detection in an earlier study (4).

TABLE 2 Numbers of vaccinia virus and host accessions detected in tryptic digestion products of two vaccinia virus virion preparations (sucrose- or tartrate-gradient purified) at the 5% and 1% FDR thresholds[a]

Virion prepn (FDR threshold)	No. of accession nos. detected		
	Vaccinia virus	Host	Ratio[b]
Sucrose (5%)	152	2,050	13.5
Sucrose (1%)	147	1,247	8.5
Tartrate (5%)	173	3,808	22.0
Tartrate (1%)	168	2,889	17.2

[a] The search taxonomy encompassed all 230 vaccinia virus WR entries in Swiss-Prot of the form XXX_VACCW. This set includes all annotated vaccinia virus WR ORFs in UniProt and all 211 unique VACWR-numbered ORFs from the vaccinia virus WR reference genome with the exception of VACWR053.5/F14.5L. Hits to the common contaminants' database (Materials and Methods) were filtered out prior to this table.
[b] Ratio of total protein hit counts, host/vaccinia virus.

From the combined studies described above, a total of 188 UniProt vaccinia virus protein accession numbers were identified within an FDR threshold of 5% (186 of these having a "VACWR" designation in the WR reference genome). These 186 represent >88% of a theoretical vaccinia virus proteome of 211 unique VACWR-numbered ORFs. Protein products from the remaining 25 vaccinia virus WR VACWR-designated ORFs (see Table S3 in the supplemental material) do not appear to have yet been detected, at least in MS studies of the virion and infected-cell proteomes. Of the 25 ORFs, 19 are located close to the genome termini, which are prone to genome plasticity, contain many secreted proteins that could escape a packaged/intracellular proteome, and have historically been prone to sequencing errors and/or they are unusually short ORFs. All but one has a UniProt annotation status of "predicted"/"inferred" or "uncharacterized." Strikingly, all but six fall into clusters of two or three contiguous ORFs in the genome.

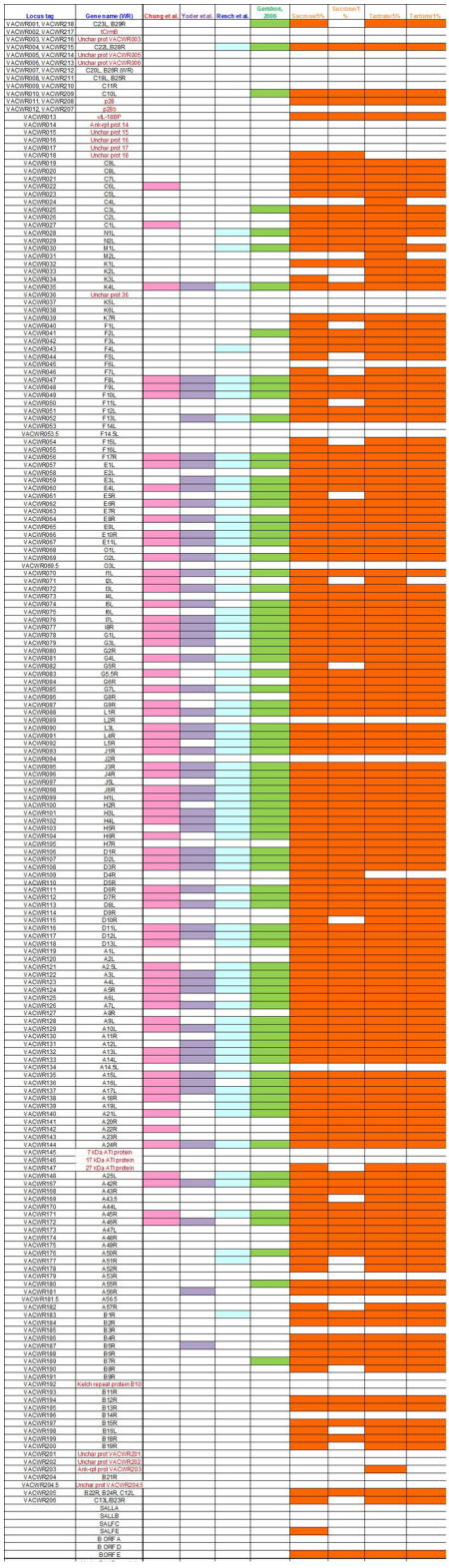

FIG 1 Progressive saturation of the viral proteome with successive analyses of virion preparations. Visual impression based on Table S2 in the supplemental material. Colors indicate the studies as follows. The results of this study are shown in orange. Other colors indicate earlier studies (2006 to 2008), either published (pink for Chung et al. [4], mauve for Yoder et al. [2], and light blue for Resch et al. [3]) or unpublished from the author's lab (green). Unchar prot, uncharacterized protein.

MS led to the first detection of gene expression products from 27 ORFs that are annotated in UniProt as either "Predicted," "Uncharacterized," "Inferred," or "Hypothetical" (see Table S4 in the supplemental material), including one as short as 39 aa. These proteins are either packaged or contaminants in the virion preparations. Included in this group were YVAT_VACCW and YVBE_VACCW, two short ORFs located within other ORFs ("ORFs-within-ORFs") present within the vaccinia virus right terminal HindIII B fragment (33). Of these proteins, YVBE_VACCW, the 91-aa product of "B ORF E," was detected in both sucrose and tartrate virion preparations, with a high Mascot score and within the highest confidence (1% FDR) threshold employed (Table S5).

The finding of gene expression products from annotated short ORFs-within-ORFs, above raised the possibility of gene expression products from additional short ORFs that had never been publicly annotated. We therefore searched the "deep" sucrose and tartrate MS data sets (discussed above) against a database generated from six-frame translations of vaccinia virus genomic DNA. This led to the confident identification, in the tartrate MS data set, of peptides from two additional ORFs (see Fig. S1 in the supplemental material). One, a 95-amino-acid open reading frame (B ORF C), is publicly annotated for the Copenhagen strain of vaccinia virus (YVBC_VACC [Swiss-Prot/UniProt]), but not for the WR strain used here. It overlapped with ORF B2R at the right end of the vaccinia virus genome on the opposite strand and was frameshifted (Fig. S1). The other, a 57-amino-acid open reading frame, overlapped with the 5′ end of ORF B29R/C23L, the terminal-most gene of the vaccinia virus inverted terminal repeats, on the same strand as B29R/C23L but frameshifted. As far as we are aware, this 57-residue ORF has never been publicly annotated.

Which proteins are packaged? From the numbers of proteins identified (Table 2), it seemed that the proteomes of the two virus preparations extended well beyond packaged proteins and into fields of contaminants. Taking the Mascot protein score as an approximate surrogate for protein abundance, database search results were ranked by descending Mascot protein score, and the resulting rankings were split according to whether the protein was from a vaccinia virus protein or a host protein (Fig. 2). Host proteins had predominantly lower ranking numbers than vaccinia virus proteins (Fig. 2), and therefore likely represent, overwhelmingly, a field of contaminants. However, since low-abundance packaged proteins may overlap in abundance with high-abundance contaminants, it was unclear where the *y* axis of Fig. 2 might be appropriately thresholded to distinguish packaged proteins from nonpackaged proteins.

To address which proteins are actually packaged within the virion, we exploited the orthogonality in virus banding methods used for the two virion preparations, namely, nonequilibrium rate-zonal velocity sedimentation ("sucrose") and equilibrium buoyant density isopycnic banding in a potassium tartrate gradient ("tartrate"). While nonpackaged proteins may preferentially contaminate one preparation or the other, packaged proteins were expected to show proportionality. Tryptic digestion products of the two virion preparations were therefore differentially isotope labeled, followed by quantitative MS. Figure 3 shows profiles of the resulting quantitation ratios for proteins quantitated from multiple peptides based on Table S6 in the supplemental material. The histogram for virus proteins was bimodal (Fig. 3), with a sharp peak centered on a tartrate/sucrose quantitative ratio bin of 0.25 to 0.5 ("< -1"), bounded by two black broken vertical lines,

TABLE 3 Vaccinia virus proteins whose detection required or was favored by nontrypsin proteases or CNBr

Gene	Protein length (aa)	Potential cleavage sites[a]	Detection	Reagent	Description (from UniProt)[b]	No. of peptide species	Best Mascot protein score	Best peptide expectation score
C19L/B25R	112	6M, 7K, 6R	Required	CNBr	Truncated ankyrin repeat protein	One	42	0.0016
C11R (VGF)	140	8D, 4E, 2K, 9R	Required	AspN	Vaccinia virus growth factor	One	31	0.0058
F6L	74	3M, 5K, 1R	Required	CNBr-trypsin	Inferred from homology	One	45	4.6E−4
F14R	73	13D, 8E, 1K, 1R	Required	AspN	Protein inferred from homology	Three (nested)	118	6.1E−06
A53R	103	3M, 6K, 6R	Required	CNBr	Truncated secreted TNF receptor-like protein, predicted to be inactive	One	68	4.50E−07
YVAT	81	2M, 1K, 3R	Required	CNBr	Uncharacterized 8.9-kDa protein	One	19	0.016
I2L	73	5D, 3E, 4K, 0R	Favored by	AspN	Late membrane protein with probable role in virus entry (32)	Two	203	2.1E−6
			Favored by	GluC		One	36	0.0044
			Favored by	CNBr		Two	320	8.10E−06
			Favored by	CNBr-trypsin		Three	536	1.10E−07

[a] Counts of potential cleavage specificity residues.
[b] TNF, tumor necrosis factor.

and a second peak centered at higher quantitative ratios coinciding more closely with the single major peak for the host proteins. The first vaccinia virus peak was clearly enriched in structural proteins, membrane proteins, and enzymes that are well established in the literature as being virion resident (Table S6, red font). The reason this peak is not centered precisely at 1:1 (i.e., at the adjacent bin, "< 0′) is discussed in the Table S6 legend.

The histogram of Fig. 3 permitted some predictions. First, for ratios between the two black broken vertical lines in Fig. 3, vaccinia virus proteins quantitated on the basis of a single peptide (not shown) may also be virion resident, albeit these are probably lower-abundance proteins whose relative quantitation is less reliable. Second, the majority of vaccinia virus accessions outside the black broken vertical lines likely represent nonpackaged virus proteins from the infected cell that accompany host cell contaminants (albeit a trailing right shoulder of the packaged-protein peak in Fig. 3 may also fall outside the black broken vertical lines). Third, cellular proteins falling within the black broken vertical lines may be candidates for packaged host cell proteins.

The experiment was repeated four times, using various, distinct pairs of virus preparations. From the resulting five experiments 58 vaccinia virus accessions were consistently found within the packaged region in all experiments (see Table S7 in the supplemental material). Sixteen additional vaccinia virus accessions considered second-tier candidates for packaging were found. Of these 16, 11 (A18R, A6L, DNLI, DUT, I1L, I3L, VLTF2, VPK1, E2L, PROF, and GLRX1) lay outside the packaged region in one experiment but within the packaged region in multiple others, while the remaining five (F12L, I5L, I6L, RP18, and A49R) were within the packaged region but were detected in only one experiment. The former could be proteins whose packaged amounts are unregulated or, alternatively, persistent contamination. The latter are likely to be low-abundance proteins. Proteins falling outside of the packaged region in multiple experiments were discounted. From this analysis, the overall number of packaged vaccinia virus proteins is concluded to be between 58 and 74. The remaining vaccinia virus accessions in Table S7 are considered nonpackaged proteins that contaminate virion preparations from the infected cell. These included the external scaffold protein D13L, considered to not be packaged (it is considered to form an external assembly scaffold) yet found in all but one of the virion MS studies so far (Table S7).

Table S8 in the supplemental material shows host proteins found in the "packaged" region of the quantitation histogram in the five experiments. A total of 82 host proteins were always found within the "packaged" region, and 63 of these 82 were found in multiple experiments (Table S8). The set of 63 host proteins was relatively rich in proteins involved in vesicular transport/protein trafficking including RABs. Since the identified RABs are functionally diverse and found in a variety of membrane compartments in the uninfected cell, they may be persistent contaminants of vaccinia virus preparations that may cosediment with virus comparably in both tartrate and sucrose gradient purification schemes such as, perhaps, exosomes or other vesicles. The second richest functional group was heat shock chaperones and associated proteins, consistent with prior findings of the importance of the stress response in vaccinia virus infection (34, 35).

Nested, noncanonical termini in vaccinia virus proteins. In a recent virion phosphoproteome analysis (22), semitryptic peptides (tryptic at one end only) were identified with high confidence among tryptic digestion products of sucrose-purified vaccinia virus virions, raising the possibility that virions may contain substantial amounts of "nicked" protein. To better understand whether "nicked" proteins might be integral to the biology of the virus, sucrose and tartrate virion preparations were digested with trypsin or alternative proteases, followed by nanoLC-MS/MS (see Table S9 in the supplemental material). In each case, a substantially higher proportion of semicanonical peptides was observed from vaccinia virus than from host peptides in the same sample (Table S10), and over all experiments, a mean of 7.6 semicanonical peptide species were observed per vaccinia virus accession versus a mean of just 1.8 per host protein in the same data sets. Moreover, while substantial groups of vaccinia virus semicanonical peptides were nested (Table S9), almost all of the host semicanonical peptides were nonnested "orphans" (Table S9 and data not shown).

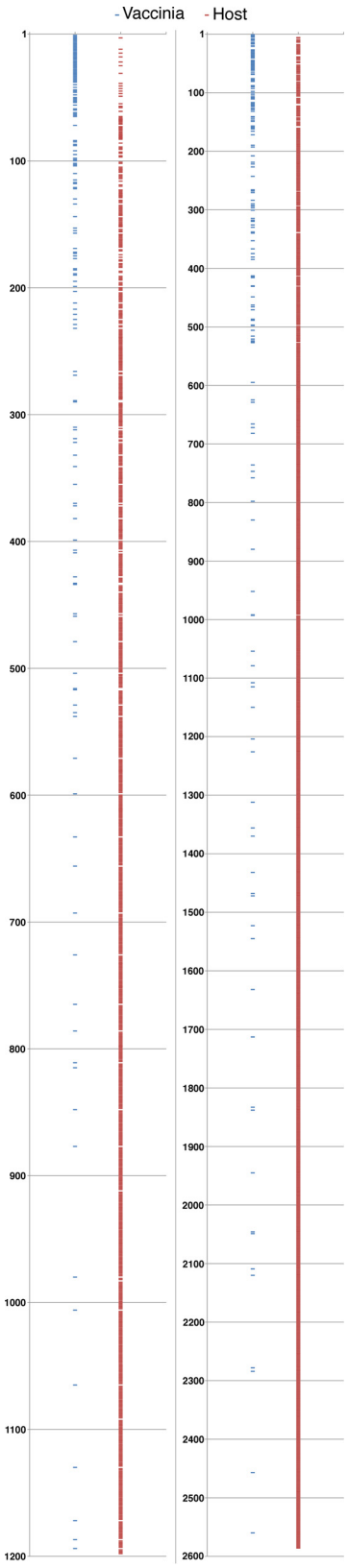

FIG 2 Confidently identified vaccinia virus and host proteins as a function of proteome depth (*y* axis) in the sucrose (left) and tartrate (right) virion preparations. Data sets (with the threshold set at the 1% FDR level) were ranked by descending Mascot protein score ($y = 1$ representing the protein ranked first, with the highest Mascot score). For each data set, ranking numbers were split into two groups, namely, "_VACCW" (blue) and human (red). Host proteins had predominantly lower ranking numbers than vaccinia virus proteins (i.e., lower abundance, or greater proteome depth).

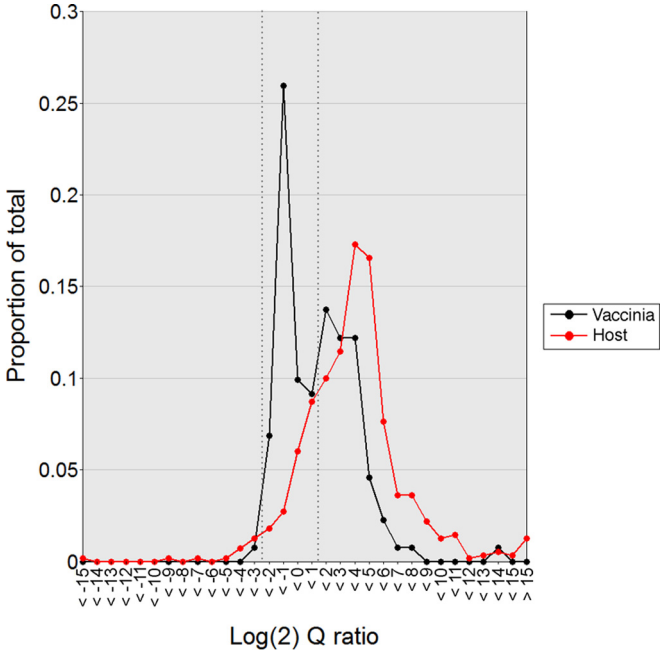

FIG 3 Line histogram showing relative quantitation of proteins present in sucrose- versus tartrate-purified vaccinia virus WR virion preparations on the basis of peptide differential isotope labeling. Only proteins quantitated on the basis of multiple peptides are shown. Vaccinia virus proteins are shown in black, and host proteins are shown in red. The $\log_2$ quantitation ratio (Q ratio) (tartrate/sucrose) is shown on the *x* axis. For example, "< -1" indicates a tartrate/sucrose ratio of 2^{-2} to 2^{-1} (0.25 to 0.5). Protein counts in bins as a proportion of all proteins in the histogram are shown on the *y* axis. Proteins in bins falling between the two black broken vertical lines were considered packaged. In the chosen approach, the more orthogonal the two preparation methods are, the more informative the experiment.

To address whether the noncanonical peptide termini may have arisen from random protein nicking during virion isolation and/or laboratory procedures, peptides were aligned from experiments involving the two distinct virion preparations (arising from distinct cell lines in different labs, prepared via distinct purification procedures, Table 1), four distinct laboratory proteases (trypsin, ArgC, GluC, or AspN), and different MS inlet voltages to control for fragmentation during MS. Results showed a substantial coincidence of noncanonical ends between virion preparations and proteases. Taking protein A26L as an example (Fig. 4; see also Fig. S2 in the supplemental material), 35% of all semitryptic peptides were common to the two virion preparations and 50% of the noncanonical ends generated in GluC, ArgC, and AspN digestion products were shared in common with tryptic peptides. Dissolution of virions followed by MS of the resulting naturally occurring large peptides directly, in the absence of any laboratory protease treatment, led to the confirmation of a number of noncanonical termini (Fig. 4 and Fig. S2). Combining all data (discussed above), the majority of vaccinia virus proteins had a high density of nick sites along the protein molecule (Table S11), while

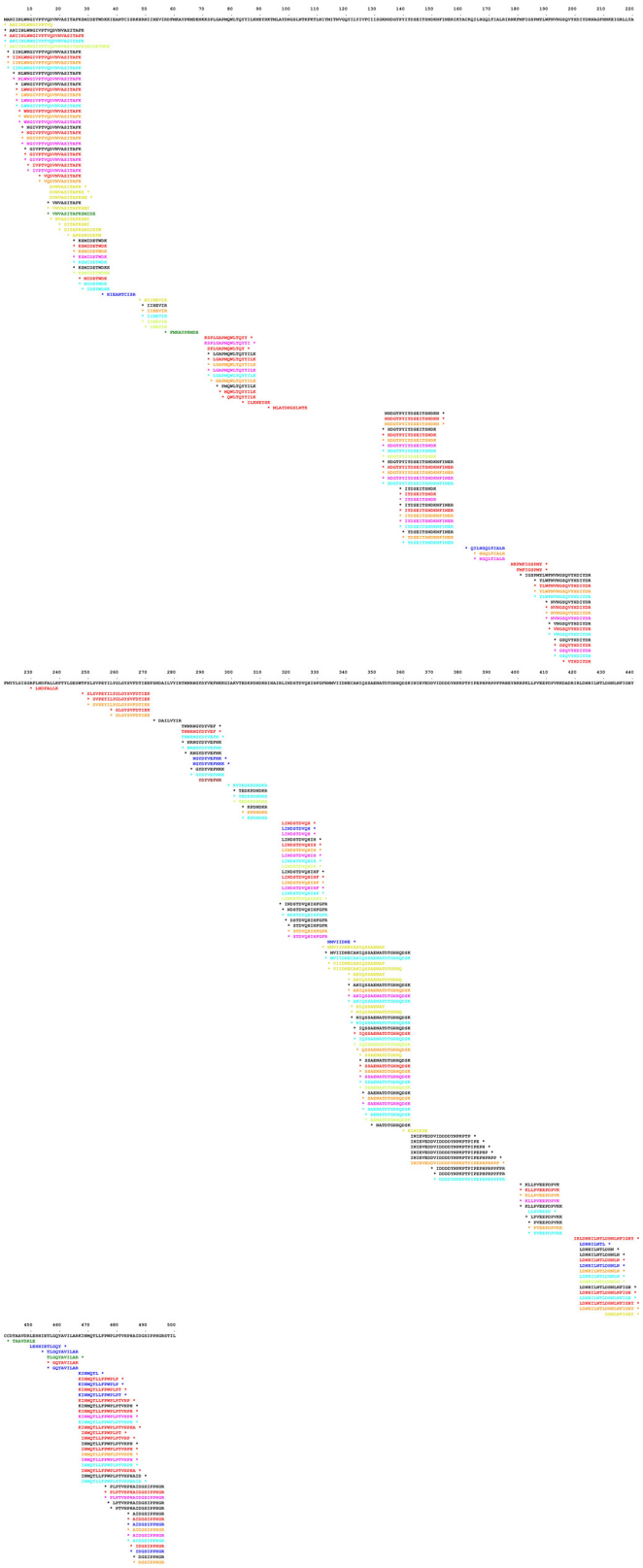

FIG 4 Semicanonical peptides covering vaccinia virus protein A26, in miniature (see Fig. S2 in the supplemental material for a full-size representation). Color coding is by experiment (Fig. S2 legend). The noncanonical terminus of each peptide is indicated with an asterisk.

the frequency of nicks per molecule for host proteins in the same samples was typically much lower and followed a very broad distribution. Moreover, the observation, within unitary nested series, of interleaved noncanonical termini from distinct experiments and different virus preparations with distinct histories (Fig. 4 and Fig. S2) suggested that partial exoproteolysis had occurred prior to laboratory manipulation and irrespective of virus source. Overall, the bias toward virus proteins and the observation of common noncanonical breakpoints irrespective of laboratory conditions, ions in which these termini appear, or virus source argued for the action of a virion-targeted (exo)protease. Protein nicking followed by exoproteolysis may be, therefore, intrinsic to the biology of infection. Noncanonical termini were not obviously flanked by a preferred amino acid (data not shown).

Since extensive virion protein degradation has not been an obvious feature of past SDS-PAGE/immunoblotting studies, we attempted to estimate the proportion of the molecules of each virion protein that are nicked, taking the best Mascot score for each unique peptide sequence as a surrogate for peptide abundance. The Mascot score distributions for canonical and noncanonical peptides in a typical tryptic peptide data set were indistinguishable (Fig. 5), suggesting that canonical and noncanonical peptides occupied the same abundance range. This suggested that, very approximately, 50% of protein molecules may be nicked in intracellular virion preparations, albeit a truly quantitative estimate is hard to obtain via the comparison of chemically nonidentical peptides.

Intravirion kinase activation. In a recent study (22), sites phosphorylated upon intravirion kinase activation *in vitro* were identified via quantitative MS. Virion tryptic phosphopeptides were quantitated before/after intravirion kinase activation to identify those with higher (or lower) intensity in mass spectra after activation. Changes in relative intensity were attributed to changes in phospho-site occupancy. This experiment, with limiting amounts of virus, was vulnerable to some standard challenges in quantitative MS (accurate model fitting to spectral peaks, spectral interference, noise, and ratio compression), along with challenges applicable to modified peptides, namely, the need to normalize phosphopeptide intensities to intensities for the corresponding nonphosphopeptides (the latter not necessarily being detected in the experiment), and the reconciliation of distinct peptide species containing the same phosphosite. Here, in a series of new experiments, vaccinia virus intravirion kinase activation was reexamined by taking a direct approach that obviated quantitative MS, namely, virion incubation with isotopically labeled (^{18}O-)ATP followed by phosphoproteome analysis. ^{18}O-marked phosphopeptides, which arise from new phosphorylation events only, can be identified via regular database searching without recourse to quantitative spectral intensity fitting.

Moreover, the new experiments allowed a deeper and broader analysis of virion phosphorylation in general via the use of two distinct virion preparations and more-advanced MS instrumentation. As a result, the overall size of the phosphoproteome expanded from 189 unique sites (22) to 370 unique sites in vaccinia virus proteins within the virion preparations (see Table S12 in the supplemental material). Many of the new sites arose exclusively from the lower-purity tartrate preparation analyzed here for the first time and were attributable to vaccinia virus proteins not detected at all in the earlier virion phosphoproteome. These proteins are considered unlikely to be packaged. Nonetheless, 268 of the

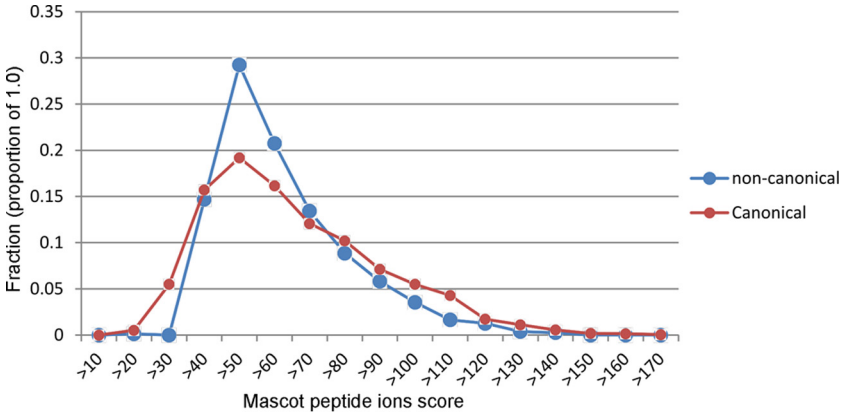

FIG 5 Line histograms showing distribution of best Mascot score per unique peptide sequence, for fully tryptic (canonical) and semitryptic (semicanonical) vaccinia virus peptides identified in the trypsin-digested sucrose virion preparation with the threshold set at the relatively stringent 1% FDR level.

370 unique sites were from within the 74 packaged virion proteins identified in Table S7. Even among packaged proteins, however, the possibility that nonpackaged or prior-to-packaging versions with distinct phosphorylation patterns exist in the infected cell cannot be excluded. Moreover, the sucrose and tartrate preparations may exhibit distinct virion phosphorylation patterns as a result of their distinct host cell and infection/growth conditions (Table 1). In addition to new sites of phosphorylation, previously reported phosphosites (22) were confirmed in new (alternative) peptide contexts (such as phosphopeptides with skipped tryptic digestion sites), and previously identified phosphopeptides were detected with improved scores.

A number of multiply phosphorylated peptides were detected for the first time where, previously, the closely spaced sites were detected only as monophosphopeptide positional isomers. The finding of new multiphosphopeptides therefore suggested the occurrence of phosphorylation clusters ("hot spots") encompassing multiple and alternative phosphorylation patterns within a localized protein region as opposed to, simply, the ambiguous software assignments of a single phosphorylation event. These phosphorylation clusters may comprise a form of "phosphorylation code" for the virion. Observation of phosphorylation in four WV proteins (A33R, A36R, B5R, and F12L), all exclusively in tartrate-purified virus preparations, indicated that tartrate preparations of vaccinia virus WR contained WV.

With regard to intravirion kinase activation, a total of 29 ^{18}O-phosphate-containing phosphopeptide species were detected, representing up to 23 sites of phosphorylation within nine vaccinia virus proteins (Table 4; see Table S12 in the supplemental material). Of the phosphopeptides previously identified as *in situ* products of intravirion kinases via quantitative MS (22), 50% were confirmed here (Table 4). This represents very good agreement, given that the prior study was by no means comprehensive (the prior data set was small, containing only clearly quantifiable peptides), and given the substantial amount of nonoverlap in the sets of phosphopeptides identified in the prior and current studies. The currently identified set of intravirion kinase substrates was more substantial (Table 4), consistent with the sensitivity of the new approach, though insufficiently large to identify a clear consensus sequence for the phosphorylation site.

Even after intravirion kinase activation, virion phosphoproteomes were overwhelmed by preexisting ^{16}O phosphorylation sites (see Table S12 in the supplemental material). With just one exception, all of the ^{18}O-containing phosphopeptides (Table 4) had ^{16}O counterparts (Table S12), demonstrating the presence, within the virion population, of prephosphorylated versions of phosphorylation events attributable to virion activation. These could represent distinct virus populations or distinct protein populations within any one virion. An alternative model that cannot be discounted would be partial dephosphorylation followed by rephosphorylation during virion kinase activation.

Within multiply phosphorylated peptides, multiple ^{18}O phosphates were never observed within the same peptide. Rather, within ^{18}O-containing multiphosphopeptides, a single ^{18}O phosphate was combined with ^{16}O phosphates at other positions. This suggested that intravirion kinase activation unleashes targeted phosphorylation events, perhaps terminal events among concerted phosphorylation cascades. With regard to the functions of proteins shown to be ^{18}O phosphorylated upon intravirion kinase activation, the clear phosphorylation of RAP94 and RP19 was consistent with the known roles of these proteins in intravirion early gene transcription. The intravirion phosphorylation of VPK2 may activate or modulate its protein kinase activity.

Blind modification search. Having investigated phosphorylation as a biological protein modification (discussed above [22]), data sets were trawled more broadly for protein modifications. Tryptic digestion products of sucrose- and tartrate-purified virions were each fractionated (via SCX), and the resulting fractions were subjected to nanoLC-MS/MS. All masses in the 1,351-member UniMod database were tested for their ability to confer peptide sequence-spectrum matches when added to masses of peptide precursors containing modifiable positions. The results of such searches were reported with a FDR threshold at the relatively stringent 1% FDR level.

With the sucrose preparation, modifications scoring better than the 1% FDR threshold were found among 132 vaccinia virus proteins, with substantial variation among proteins in the mean density of putative modifications per residue. These observed modification densities are likely attributable to protein abundance in the virion preparation, with higher abundance allowing the detection of more weakly ionizing modified peptides or sites with lower occupancy. Thus, structural protein P4b had one of the highest observed modification densities. Some modification masses were more easily interpretable than others, with higher

TABLE 4 All ^{18}O phosphopeptides detected here, excerpted from Table S12 in the supplemental material[a]

Accession	Phosphopeptide	Position	Prior
A14_VACCW	VSGVIHTNHSDISMN	85	✓
A14_VACCW	VSGVIHTNHSDISMN	88	
A14_VACCW	VSGVIHTNHSDISMN	82;85;88	
A14_VACCW	VSGVIHTNHSDISMN	82;88	
A14_VACCW	VSGVIHTNHSDISMN	85;88	
A19_VACCW	TTVIDDDDDCMTCSACQSK	36	
A19_VACCW	TTVIDDDDDCMTCSACQSK	32;36	✓
A19_VACCW	LVKISDITK	42	✓
F17_VACCW	QVPFMRTDMLQNMFAANR	81	
F17_VACCW	DNVASRLLN	97	
G7_VACCW	GYKTDGAVTSPLTGNNTITTFIPISASDMQK	304	
G7_VACCW	TDGAVTSPLTGNNTITTFIPISASDMQK	304	
G7_VACCW	TDGAVTSPLTGNNTITTFIPISASDMQK	305	
G7_VACCW	TDGAVTSPLTGNNTITTFIPISASDMQK	308	
G7_VACCW	GYKTDGAVTSPLTGNNTITTFIPISASDMQK	312	
G7_VACCW	TDGAVTSPLTGNNTITTFIPISASDMQK	312	
L1_VACCW	NMCSADADAQLDAVLSAATETYSGLTPEQK	58	
P4A_VACCW	NLNMTDGDSVSFDDE	881	
P4A_VACCW	NLNMTDGDSVSFDDE	885	
RAP94_VACCW	NSDLVSSFNAELEPEIK	151	
RAP94_VACCW	NSDLVSSFNAELEPEIK	152	
RP19_VACCW	IVESASTHIEDAHSNLK	49	✓
RP19_VACCW	IVESASTHIEDAHSNLK	50	✓
RP19_VACCW	IVESASTHIEDAHSNLK	47;49	
RP19_VACCW	IVESASTHIEDAHSNLK	49;50	
VPK2_VACCW	GVANDSSPEYQWMSPHR	8	
VPK2_VACCW	GVANDSSPEYQWMSPHR	7;8	
VPK2_VACCW	GVANDSSPEYQWMSPHR	7;15	
VPK2_VACCW	GVANDSSPEYQWMSPHR	8;15	
P4A_VACCW	✖	743	
A6_VACCW	✖	118/121	
A13_VACCW	✖	48	
A13_VACCW	✖	61	
VP8_VACCW	✖	220	

[a] The accession numbers are shown in the leftmost column. In the Phosphopeptide column the ^{18}O and ^{16}O phospho positions are indicated in red and green, respectively. In the Position column, the position(s) of red/green site(s) within the protein sequence are given. A check mark in the Prior column indicates agreement with the published quantitative MS study (22). The last five rows (marked "✖" in the Phosphopeptide column) show proteins considered substrates of intravirion kinases previously (22) but not reconfirmed here.

modification masses more diagnostic of a specific modification. Interpretable modification masses included a broad selection of apparent metabolite labels on cysteine and lysine side chains (data not shown). A number of modifications were mundane (e.g., oxidation) or not necessarily reflective of the intact protein (e.g., cation binding). Notably absent was protein ubiquitination. Here, we deliberately eschewed the standard treatment of tryptic peptide preparations with iodoacetamide (Materials and Methods), since the resulting promiscuous carbamidomethyl modification is isobaric with the trypsinized ubiquitin adduct Gly (K). Some specific classes of modification are discussed below:

Protein fatty acylation. We first examined fatty acylation as one of the known posttranslational modifications of vaccinia virus (see the introduction). One of the best known acylations in vaccinia virus is the N-terminal myristoylation of L1 protein (7, 8, 36). In the current study, a myristoylation mark was found at the N-terminal Gly of the initiator methionine-demethionylated N-terminal tryptic peptide of vaccinia virus protein L1R (sucrose preparation) and nowhere else in this proteome. In the tartrate preparation, this mark was found at the N-terminal Gly of protein E7R and nowhere else. E7R is also known to be myristoylated (9). These findings highlighted the following two significant points. (i) Protein modification marks demonstrated via non-MS approaches could be detected using our MS approach without false-positive results. (ii) Different virion preparations yielded differential detection of known modifications. For apparent myristoylproteins G9R and A16L (see the introduction), neither myristoylation nor the unmodified N-terminal peptide was detected, although in general, the partial or full loss of myristate or *N*-myristoylglycine by hydrolysis (37) under the acid conditions of LC-MS/MS cannot be fully discounted. Despite reports of vaccinia virus protein labeling with palmitate in cell culture (7, 11–17; see the introduction), in neither of the two virion preparations were protein palmitoylation or prenylation detected (data not shown). For palmitoylation at least, the lability of the *S*-palmitate thioester linkage to conditions of sample preparation and MS is likely a consideration, in addition to peptide hydrophobicity.

Protein N-terminome. With the above in mind, we proceeded to collate the N-terminome of the virion. N-terminal peptides were found for 30 vaccinia virus proteins of which just three were found in exclusively unmodified form. The remainder showed methionine loss and/or N-terminal acetylation (see Table S13 in the supplemental material). Of these 30 proteins, 26 showed N-terminal acetylation, consistent with the 70 to 90% N-terminal acetylation rate for proteins of the host cell (38). Overall, results from sucrose and tartrate preparations were largely in agreement (Table S13 legend).

Additional phosphorylation sites. The phosphopeptides identified above (see Table S12 in the supplemental material) arose from phosphopeptide-specific enrichment. Up to 26 new phosphosites were found in the sucrose and tartrate blind modification search data sets (Table S14), raising the maximum number of unique phosphosites over the two virion preparations to 396. The new data included 10 new multiple phosphorylation combinations.

Cysteine modification. For the blind modification experiments, cysteine residues were not capped prior to MS, affording an opportunity to assess natural cysteine modifications. Since the commonly used cysteine capping reaction with iodoacetamide is promiscuous (reacting with Lys side chains for example) and is isobaric with Gly(K), the tryptic stub of ubiquitinated Lys-containing peptides, it may be no coincidence therefore that our overall modification data set did not include ubiquitination (data not shown). In our blind modification data sets, the overwhelming majority of cysteines were modified in some manner, with very few cysteines detected in exclusively unmodified form (see Table S15 in the supplemental material). Cysteine was second only to lysine in the diversity of modification types detected (data not shown). Table 5 shows the most common types of mass increase associated with cysteine modification. Since the overall extent of glutathionylation was comparable in virus and host proteins in the same preparations (Table S16), there was apparently no bulk glutathionylation of vaccinia virus proteins. However, this did not rule out the possibility of narrowly targeted glutathionylation.

As a reversible modification, *S*-glutathionylation may be subjected to positional scrambling during preparation for MS. Nonetheless, the odds seem to be against this having occurred in bulk. The most likely outcome of picking 47 cysteines (see Table S17 in the supplemental material) randomly from a total cysteine count

TABLE 5 Four most common gain-of-mass cysteine modifications among vaccinia virus proteins in the sucrose and tartrate virion blind modification data sets[a]

Cysteine modification	Modified mass	No. of PSMs[b]			
		Sucrose		Tartrate	
		VV	Host	VV	Host
Glutathione (C)	305.07	75	26	61	90
Trioxidation (C)	47.98	70	56	38	71
Cyano (C)	25	57	89	19	19
Nitrosyl (C)	28.99	37	114	8	66

[a] Four most common (by counting of peptide spectral matches [PSMs]) gain-of-mass cysteine modifications in vaccinia virus proteins in the sucrose and tartrate virion blind modification data sets. Trioxidation = cysteic acid. Gain-of-mass modifications exclude, for example, Cys→Ala (SH loss).
[b] PSMs, peptide spectral matches; VV, vaccinia virus.

of 804 (Table S15), then picking 41 from a total of 929 (tartrate), would be no significant amount of positional overlap in *S*-glutathionylation between the sucrose and tartrate data sets. In contrast, 35% of all detected positions of *S*-glutathionylation were common in the sucrose and tartrate data sets (Table S17). Nearly all sites, whether unique or common, scored higher than our benchmark modification, namely, L1 protein myristoylation (Fig. S3), suggesting that our identification was reliable for the majority of *S*-glutathionylation sites detected (Fig. S3).

Glycosylation. Affecting perhaps the greatest number of vaccinia virus proteins (up to 70 over the two virus preparations) and among the most diverse of the modification types was glycosylation, N linked and O linked (see Table S18 in the supplemental material). As with other modification types, these 70 proteins may not all be packaged. Putative glycan structures were assigned on the basis of modification mass and position, but their identities are quite tentative for several reasons including the following: (i) increased variety of potential isomers with increasing modification mass (glycans being among the largest) and a greater potential for the assigned modification mass to be the sum of multiple, lower mass modifications and (ii) the incomplete development of glycans within the UniMod database with ambiguity, for some glycan entries, in whether they are N linked, O linked, or both. Importantly, our approach was informatic only, involving no experimental analysis of enriched glycopeptides.

With the above in mind, regarding N-linked glycosylation results, blind modification searches for the sucrose data set yielded 34 combinations of apparent N-glycan and peptide and attachment site, within 14 vaccinia virus proteins (A17L, A26L, A4L, E8R, F9L, G9R, L1R, L3L, NTP1, P4A, P4B, RAP94, RP147, and VP8 [see Table S19 in the supplemental material]). Of these proteins, A17L, A26L, and L1R are established membrane proteins, as are E8R (39) and F9L (40). G9R is presumed to be membrane associated, as a myristoylated member of the poxvirus entry-fusion complex (41). For the structural proteins P4A, p4B, A4, and VP8, trace glycosylation may have been detected experimentally due to their relatively high abundance. Interestingly, the data set included four transcription proteins (L1, NTP1, RAP94, and RP147), whose modifications were specifically denoted "PhosphoHex(2)." This refers to either the linkage of a disaccharide to the phosphate of phosphorylated serine (pS) or phosphorylated threonine (pT) or, perhaps pertinent to the modified NTP1, RAP94, and RP147 peptides, which do not possess S/T residues, the linkage of an N-linked sugar to another sugar via a phosphodiester (42). This is an example of microbial eukaryotic phosphoglycosylation, as reported in some slime molds and unicellular parasites (42). Although mannose-6-phosphate modification has a role in the targeting of lysosome-resident enzymes to the lysosome in mammalian cells (43), this appears to be a modification of more-complex (high-mannose) glycans, that are exclusively N linked (43). Overall, PhosphoHex-modified peptides [PhosphoHex and PhosphoHex(2)] seemed quite plentiful in blind modification search results (Table S20).

To determine whether a combination of phosphorylation and glycosylation at distinct sites within a peptide might have been misassigned as PhosphoHex(2), a search of the sucrose "deep" data set was conducted specifying Hex (ST), Phospho (ST), PhosphoHex(2) (N), and PhosphoHex(2) (ST) as competing variable modifications. Results (see Table S21 in the supplemental material) showed that the majority of modified vaccinia virus peptides were exclusively modified with either PhosphoHex(2) (ST), PhosphoHex(2) (N), Phospho (ST), or Hex (ST), and very few peptides were identified with multiple, alternative modifications. Many of the uniquely PhosphoHex(2)-modified peptides scored with very high confidence. This experiment therefore supported the contention that the detection of phosphoglycosylated vaccinia virus proteins was not artifactual.

In only 3 of the 34 N-glycopeptides indicated above (see Table S19 in the supplemental material) was the glycan assigned to a canonical NX(S/T) motif (44, 45) though 10 of the peptides contained NX(S/T) elsewhere, suggesting possible informatic mislocalization. For six of the peptides, the glycan was assigned to NXC. In global studies of cellular glycomes, NXC has been shown to be used for N-linked glycosylation, though in only ~1% of instances (46, 47). The motif (S/T)XN (48) appeared four times in the listing but not at the assigned site. The 18 remaining unique glycopeptides included some of the highest-scoring members of the 34-member set (Table S19) arguing against their inclusion arising from inappropriate threshold levels. Among these 18 glycopeptides, the assigned attachment site fell in the context of NXY for 5 peptides, NI for an additional 3 peptides, or the NCN, NXG, or NXL. These sequences accounted for all but 3 of the remaining 18 peptides.

In addition to N-linked glycosylation, the virion proteome seemed rich in O-glycoforms (see Table S18 in the supplemental material). Perhaps the most abundantly O-glycosylated protein was structural protein p4b, showing >35% saturation of all S or T residues with some form of apparent O-glycan (Table S22) along with many instances of alternative glycoform masses at identical positions (most notably at position T100). While alternative glycans at the same site with dissimilar compositions clearly represent alternative p4b molecules (within either the same or different virions), overall, partial glycan fragmentation and/or loss during MS cannot be discounted. It can be concluded that there is abundant O-linked glycosylation among vaccinia virus proteins, though it is hard to draw more-definitive conclusions without additional experimental data.

DISCUSSION

In this study, we have characterized the vaccinia virus virion proteome at the level of primary (covalent) structure via analytical MS. By necessity and design, the sensitivity of modern MS can cover several orders of abundance dynamic range in a single ex-

periment. In this context, our two virion preparations, which comprised pure virus by virological metrics, contained products attributable to >88% of all open reading frames of the reference virus genome (Fig. 1). This was quite notable, given that the virion preparations sampled the infected cell only at late times of infection and given the absence of enrichment for secreted and other nonpackaged proteins. All eight wrapping membrane proteins (49), namely, A56R (50, 51), F12L (52), F13L (17), B5R (16, 19), A34R (18), A36R (53), A33R (15), and K2L (54), were identified unequivocally in the virion preparations (see Table S1 in the supplemental material). This was despite the relatively low propensity of most vaccinia virus strains, including WR used here, to form extracellular virus (55, 56), although intracellular wrapped virus may be undiminished. Phosphorylation was confidently detected in four of them. MS results did not, of course, reveal whether these proteins are localized exclusively in the wrapping membrane.

Our virion proteomes also verified the expression of 27 ORFs publicly annotated as "Predicted," "Uncharacterized," "Inferred" or "Hypothetical" and whose products had not previously been found in MS studies (see Table S4 in the supplemental material). These ORFs included two small previously annotated "ORFs-within-ORFs" whose expression had not previously been demonstrated and two new "ORFs-within-ORFs" identified solely by searching MS data against vaccinia virus genomic DNA as opposed to proteome-based databases (Fig. S1). One of these ORFs had been annotated in the Copenhagen strain of vaccinia virus but not in the WR strain used here, and the other had never been publicly annotated, albeit the ORF can be found in both the WR and Copenhagen strains (Fig. S1). Products of the four short ORFs were identified despite our experiments not being designed as an exhaustive screen for short-ORF expression. For example, deep peptide fractionation was applied to tryptic digestion products only, and DNA-level searching was applied to data from only two experiments. Moreover, since this was a virion sample, products from additional small ORFs may have been lost during virus preparation and/or or secreted from the host cell.

Of the 25 stubbornly silent ORFs representing the remaining 12% of the reference vaccinia virus "ORFome" (see Table S3 in the supplemental material), only 14 were recognizably present in the Copenhagen strain (Table S3) and just 10 are annotated for the Copenhagen strain in Swiss-Prot/UniProt. In particular, ORFs closer to the genome termini lacked counterparts in the Copenhagen strain. The silent ORFs tended to fall in blocks, or clusters of contiguous ORFs. Assuming accurate genome annotation, this raises the possibility that plastic regions close to the genome termini may have decayed to silence functionally, even if formally still intact at the structural level.

Due to the distinction between biological and proteomic purity (discussed above), a quantitative MS approach was taken to identify proteins that are packaged. By "packaged" we mean consistently and selectively virus associated. A quantitative comparison of proteins in the two orthogonally purified virion samples led to a set of 58 to 74 proteins that were considered to be packaged (see Tables S6 and S7 in the supplemental material). Conversely, the "nonpackaged" regions of quantitation histograms (for example, see Table S6) comprised proteins with roles in the infected cell but not in the virion such as nucleotide-metabolizing enzymes, DNA polymerase, intermediate and late transcription factors, and the external scaffold protein D13L (which is proteolytically removed during virion maturation [57] but nonetheless can be found in the majority of MS studies of mature virions [Table S1]). Sixteen proteins did not consistently fall within the packaged regions of the quantitation histograms. If packaged, then these might be "variable-stoichiomietry" proteins, able to show quantitative packaging differences between virion preparations. Alternatively, the infected cell may contain both packaged and nonpackaged versions of these proteins, with the nonpackaged portion highly represented in the cytoplasm or the virus factory but only packaged in relatively limited amounts. Another possibility would be a mixture of immature/mature forms whose relative proportions vary between virus preparations. Finally, viruses packaged in different cell lines (Table 1) or purified in different ways may be sensitive to differential loss of packaged proteins that are weakly bound.

A total of 63 host cell proteins fell consistently within the "packaged" region of the quantitation histogram in multiple experiments (see Table S8 in the supplemental material). Some of these proteins may also be packaged, though alternative possibilities may include equivalent contamination with vesicular material, nuclei or mitochondria arising, for example, from equivalent cosedimentation. Nonetheless, the experiment may be considered the most rigorous screen thus far for candidate packaged host cell proteins, and a basis for further study.

Vaccinia virus virion proteins showed extensive presence of nested, noncanonical internal termini, irrespective of laboratory treatment or source/method of preparation of virus. These termini were consistent between two distinct preparations of mature intracellular virus (MV) and between different peptide species after laboratory proteolysis (or lack thereof), and are likely present within MV inside the infected cell. It is unclear which would predominate within the virion, intact or "nicked" proteins. Mascot score distributions for noncanonical versus canonical peptides (Fig. 5) suggested comparable abundances, albeit since Mascot scoring uses a log scale, the distributions could be insensitive to peptide abundance differences. On the other hand, if, say, 50% of the molecules of a given protein were singly nicked at any one of 30 distinct sites, then the impression from SDS-PAGE or immunoblotting may be of a clean protein preparation dominated by discrete intact proteins. This would contrast with the picture arising from high-sensitivity peptide-level MS. The internal termini were suggestive of two-step proteolysis (endoproteolysis followed by exoproteolysis). In this regard, it is notable that vaccinia virus contains genes that encode and package two distinct proteases (G1L and I7L). Only the first (nicking) step would need to be regulated if the second step were concerted. While two-step proteolysis could speculatively have a role in either virus maturation or the uncoating step early during infection, the latter would presumably represent spurious activation, since virus was harvested from cells infected at a late stage.

A "blind modification" search of MS data covered all 1,351 listed modifications in the UniMod database. Modifications were assigned to MS data on the basis of modification mass alone. Among the more prominent modifications detected was apparent cysteine glutathionylation. Cytoplasmic glutathione is a known protective antioxidant, maintaining a reducing environment in the cytoplasm. *S*-Glutathionylation is also an intermediate in disulfide bond homeostasis and may have regulatory roles in protein function (58–60). Whether vaccinia virus protein *S*-glutathionylation is a product of general redox homeostasis, targeted disulfide exchange, or some regulatory pathway is unclear. Vaccinia virus

carries genes that encode two glutaredoxins, one of which is essential and promotes disulfide bond formation in specific vaccinia virus protein domains exposed to the reducing environment of the cytoplasm during virion assembly (61, 62). In the characterized vaccinia virus pathway (63–65), glutathione (GSH) does not participate directly in the flow of electrons from vaccinia virus protein sulfhydryls to the FAD electron sink. However, in general, members of the glutaredoxin family can participate in disulfide bond homeostasis in both directions (reduction as well as formation [66]), and the reductive pathway can include protein *S*-glutathione adduct formation as an intermediate (66). Despite virion assembly being the only role characterized thus far, it is conceivable that targeted disulfide formation then reversal may occur at distinct stages of the vaccinia virus life cycle, consistent with the packaging of two glutaredoxins by the virus.

Among accessions (see Table S17 in the supplemental material), L1R showed the greatest number of *S*-glutathionylation sites, marking cysteines from each of the three disulfides. The three disulfides of L1R (linking the protein's six cysteines, namely, 34 to 57, 49 to 136, and 116 to 158 [67]) are known targets of directed disulfide bond modification during the virion assembly pathway (63, 68). In the protein's three-dimensional (3D) structure, all six cysteines are apparently sequestered from solvent (67), with the greatest solvent exposure (12%) apparent for C-158. Somewhat ironically, our data set included ions representing the confident modification of all cysteines with the exception of C-158, including as many as 52 ions for the confident modification of C-57, a residue showing 0% solvent exposure in the X-ray crystal structure. This suggests some plasticity in the L1R structure, and/or the modification of its cysteines against thermodynamic barriers. The F9L protein, the other known target of vaccinia virus active disulfiding (63), was also clearly marked by *S*-glutathionylation in our data sets (Table S17).

Another modification that appeared abundantly in our blind modification data set was glycosylation. Apparent N-linked glycan attachment sites were mainly noncanonical, raising the possibility of either perturbed attachment specificity or ambiguity in our analysis. N-linked glycosylation at noncanonical sites has been observed in cellular studies (46, 47), though only extremely rarely (46). Notably for vaccinia virus, the transmembrane oligosaccharyltransferase complex responsible for N-linked glycosyl attachment is associated with the luminal side of the endoplasmic reticulum (ER) (69). Since the ER lumen is intimately linked with the earliest stages of vaccinia virus virion assembly in cytoplasmic factories, and the outer surface of the pox virion may be derived from the luminal side of the ER membrane (70, 71), it is not inconceivable that this complex may be promiscuously exposed to various vaccinia virus proteins during virion assembly under conditions of disrupted or distorted enzyme specificity. Overall, there is a clear need for experimental data to validate glycan attachment sites, and the current data provide a starting point for experimentation.

In summary, we present a comprehensive reference study that begins to reveal the protein covalent structure of the vaccinia virus virion, as a longitudinal (deep) analysis of a relatively simple proteome. Although the current study is perhaps the most penetrating thus far, it does not represent the totality of virion primary structure, and it does not even necessarily scratch the surface. Most notably, in addition to fully understanding and validating the diversity of posttranslational modifications detected here, the combination of modifications within a virion protein molecule, the diversity of proteoforms within a particle and of viroforms within a preparation are all challenges for the future.

ACKNOWLEDGMENTS

This work was supported by NIH grant 5R21AI101577 and NIH SIG 1S10OD016328.

REFERENCES

1. **Jensen ON, Houthaeve T, Shevchenko A, Cudmore S, Ashford T, Mann M, Griffiths G, Krijnse Locker J.** 1996. Identification of the major membrane and core proteins of vaccinia virus by two-dimensional electrophoresis. J Virol **70:**7485–7497.
2. **Yoder JD, Chen TS, Gagnier CR, Vemulapalli S, Maier CS, Hruby DE.** 2006. Pox proteomics: mass spectrometry analysis and identification of Vaccinia virion proteins. Virol J **3:**10. http://dx.doi.org/10.1186/1743-422X-3-10.
3. **Resch W, Hixson KK, Moore RJ, Lipton MS, Moss B.** 2007. Protein composition of the vaccinia virus mature virion. Virology **358:**233–247. http://dx.doi.org/10.1016/j.virol.2006.08.025.
4. **Chung CS, Chen CH, Ho MY, Huang CY, Liao CL, Chang W.** 2006. Vaccinia virus proteome: identification of proteins in vaccinia virus intracellular mature virion particles. J Virol **80:**2127–2140. http://dx.doi.org/10.1128/JVI.80.5.2127-2140.2006.
5. **Manes NP, Estep RD, Mottaz HM, Moore RJ, Clauss TR, Monroe ME, Du X, Adkins JN, Wong SW, Smith RD.** 2008. Comparative proteomics of human monkeypox and vaccinia intracellular mature and extracellular enveloped virions. J Proteome Res **7:**960–968. http://dx.doi.org/10.1021/pr070432+.
6. **Takahashi T, Oie M, Ichihashi Y.** 1994. N-terminal amino acid sequences of vaccinia virus structural proteins. Virology **202:**844–852. http://dx.doi.org/10.1006/viro.1994.1406.
7. **Franke CA, Reynolds PL, Hruby DE.** 1989. Fatty acid acylation of vaccinia virus proteins. J Virol **63:**4285–4291.
8. **Franke CA, Wilson EM, Hruby DE.** 1990. Use of a cell-free system to identify the vaccinia virus L1R gene product as the major late myristylated virion protein M25. J Virol **64:**5988–5996.
9. **Martin KH, Grosenbach DW, Franke CA, Hruby DE.** 1997. Identification and analysis of three myristylated vaccinia virus late proteins. J Virol **71:**5218–5226.
10. **Rodriguez JR, Risco C, Carrascosa JL, Esteban M, Rodriguez D.** 1997. Characterization of early stages in vaccinia virus membrane biogenesis: implications of the 21-kilodalton protein and a newly identified 15-kilodalton envelope protein. J Virol **71:**1821–1833.
11. **Grosenbach DW, Hansen SG, Hruby DE.** 2000. Identification and analysis of vaccinia virus palmitylproteins. Virology **275:**193–206. http://dx.doi.org/10.1006/viro.2000.0522.
12. **Child SJ, Hruby DE.** 1992. Evidence for multiple species of vaccinia virus-encoded palmitylated proteins. Virology **191:**262–271. http://dx.doi.org/10.1016/0042-6822(92)90188-U.
13. **Hiller G, Weber K.** 1985. Golgi-derived membranes that contain an acylated viral polypeptide are used for vaccinia virus envelopment. J Virol **55:**651–659.
14. **Payne LG.** 1992. Characterization of vaccinia virus glycoproteins by monoclonal antibody precipitation. Virology **187:**251–260. http://dx.doi.org/10.1016/0042-6822(92)90313-E.
15. **Roper RL, Payne LG, Moss B.** 1996. Extracellular vaccinia virus envelope glycoprotein encoded by the A33R gene. J Virol **70:**3753–3762.
16. **Isaacs SN, Wolffe EJ, Payne LG, Moss B.** 1992. Characterization of a vaccinia virus-encoded 42-kilodalton class I membrane glycoprotein component of the extracellular virus envelope. J Virol **66:**7217–7224.
17. **Hirt P, Hiller G, Wittek R.** 1986. Localization and fine structure of a vaccinia virus gene encoding an envelope antigen. J Virol **58:**757–764.
18. **Duncan SA, Smith GL.** 1992. Identification and characterization of an extracellular envelope glycoprotein affecting vaccinia virus egress. J Virol **66:**1610–1621.
19. **Engelstad M, Howard ST, Smith GL.** 1992. A constitutively expressed vaccinia gene encodes a 42-kDa glycoprotein related to complement control factors that forms part of the extracellular virus envelope. Virology **188:**801–810. http://dx.doi.org/10.1016/0042-6822(92)90535-W.
20. **Shida H, Dales S.** 1981. Biogenesis of vaccinia: carbohydrate of the hem-

agglutinin molecules. Virology **111:**56–72. http://dx.doi.org/10.1016/0042-6822(81)90653-X.
21. **Moss B.** 2006. Poxviridae: the viruses and their replication, p 2905–2946. *In* Knipe DM, Howley PM, Griffin DE, Lamb RA, Martin MA, Roizman B, Straus SE (ed), Fields virology, 5th ed. Lippincott, Williams & Wilkins, Philadelphia, PA.
22. **Matson J, Chou W, Ngo T, Gershon PD.** 2014. Static and dynamic protein phosphorylation in the Vaccinia virion. Virology **452-453:**310–323. http://dx.doi.org/10.1016/j.virol.2014.01.012.
23. **Condit RC, Moussatche N, Traktman P.** 2006. In a nutshell: structure and assembly of the vaccinia virion. Adv Virus Res **66:**31–124. http://dx.doi.org/10.1016/S0065-3527(06)66002-8.
24. **VanSlyke JK, Franke CA, Hruby DE.** 1991. Proteolytic maturation of vaccinia virus core proteins – identification of a conserved motif at the N termini of the 4b and 25K virion proteins. J Gen Virol **72:**411–416. http://dx.doi.org/10.1099/0022-1317-72-2-411.
25. **Ansarah-Sobrinho C, Moss B.** 2004. Role of the I7 protein in proteolytic processing of vaccinia virus membrane and core components. J Virol **78:**6335–6343. http://dx.doi.org/10.1128/JVI.78.12.6335-6343.2004.
26. **Byrd CM, Bolken TC, Hruby DE.** 2003. Molecular dissection of the vaccinia virus I7L core protein proteinase. J Virol **77:**11279–11283. http://dx.doi.org/10.1128/JVI.77.20.11279-11283.2003.
27. **Moussatche N, Keller SJ.** 1991. Phosphorylation of vaccinia virus core proteins during transcription in vitro. J Virol **65:**2555–2561.
28. **Chou W, Ngo T, Gershon PD.** 2012. An overview of the vaccinia virus infectome: a survey of the proteins of the poxvirus-infected cell. J Virol **86:**1487–1499. http://dx.doi.org/10.1128/JVI.06084-11.
29. **da Fonseca FG, Weisberg AS, Caeiro MF, Moss B.** 2004. Vaccinia virus mutants with alanine substitutions in the conserved G5R gene fail to initiate morphogenesis at the nonpermissive temperature. J Virol **78:**10238–10248. http://dx.doi.org/10.1128/JVI.78.19.10238-10248.2004.
30. **Senkevich TG, Wyatt LS, Weisberg AS, Koonin EV, Moss B.** 2008. A conserved poxvirus NlpC/P60 superfamily protein contributes to vaccinia virus virulence in mice but not to replication in cell culture. Virology **374:**506–514. http://dx.doi.org/10.1016/j.virol.2008.01.009.
31. **Satheshkumar PS, Moss B.** 2009. Characterization of a newly identified 35-amino-acid component of the vaccinia virus entry/fusion complex conserved in all chordopoxviruses. J Virol **83:**12822–12832. http://dx.doi.org/10.1128/JVI.01744-09.
32. **Nichols RJ, Stanitsa E, Unger B, Traktman P.** 2008. The vaccinia virus gene I2L encodes a membrane protein with an essential role in virion entry. J Virol **82:**10247–10261. http://dx.doi.org/10.1128/JVI.01035-08.
33. **Smith GL, Chan YS, Howard ST.** 1991. Nucleotide sequence of 42 kbp of vaccinia virus strain WR from near the right inverted terminal repeat. J Gen Virol **72:**1349–1376. http://dx.doi.org/10.1099/0022-1317-72-6-1349.
34. **Jindal S, Young RA.** 1992. Vaccinia virus infection induces a stress response that leads to association of Hsp70 with viral proteins. J Virol **66:**5357–5362.
35. **Hung JJ, Chung CS, Chang W.** 2002. Molecular chaperone Hsp90 is important for vaccinia virus growth in cells. J Virol **76:**1379–1390. http://dx.doi.org/10.1128/JVI.76.3.1379-1390.2002.
36. **Foo CH, Whitbeck JC, Ponce-de-Leon M, Saw WT, Cohen GH, Eisenberg RJ.** 2012. The myristate moiety and amino terminus of vaccinia virus l1 constitute a bipartite functional region needed for entry. J Virol **86:**5437–5451. http://dx.doi.org/10.1128/JVI.06703-11.
37. **Towler D, Glaser L.** 1986. Acylation of cellular proteins with endogenously synthesized fatty acids. Biochemistry **25:**878–884. http://dx.doi.org/10.1021/bi00352a021.
38. **Starheim KK, Gevaert K, Arnesen T.** 2012. Protein N-terminal acetyltransferases: when the start matters. Trends Biochem Sci **37:**152–161. http://dx.doi.org/10.1016/j.tibs.2012.02.003.
39. **Doglio L, De Marco A, Schleich S, Roos N, Krijnse Locker J.** 2002. The vaccinia virus E8R gene product: a viral membrane protein that is made early in infection and packaged into the virions' core. J Virol **76:**9773–9786. http://dx.doi.org/10.1128/JVI.76.19.9773-9786.2002.
40. **Brown E, Senkevich TG, Moss B.** 2006. Vaccinia virus F9 virion membrane protein is required for entry but not virus assembly, in contrast to the related L1 protein. J Virol **80:**9455–9464. http://dx.doi.org/10.1128/JVI.01149-06.
41. **Ojeda S, Domi A, Moss B.** 2006. Vaccinia virus G9 protein is an essential component of the poxvirus entry-fusion complex. J Virol **80:**9822–9830. http://dx.doi.org/10.1128/JVI.00987-06.
42. **Haynes PA.** 1998. Phosphoglycosylation: a new structural class of glycosylation? Glycobiology **8:**1–5. http://dx.doi.org/10.1093/glycob/8.1.1.
43. **Coutinho MF, Prata MJ, Alves S.** 2012. Mannose-6-phosphate pathway: a review on its role in lysosomal function and dysfunction. Mol Genet Metab **105:**542–550. http://dx.doi.org/10.1016/j.ymgme.2011.12.012.
44. **Hart GW.** 1992. Glycosylation. Curr Opin Cell Biol **4:**1017–1023. http://dx.doi.org/10.1016/0955-0674(92)90134-X.
45. **Aebi M.** 2013. N-linked protein glycosylation in the ER. Biochim Biophys Acta **1833:**2430–2437. http://dx.doi.org/10.1016/j.bbamcr.2013.04.001.
46. **Zielinska DF, Gnad F, Wisniewski JR, Mann M.** 2010. Precision mapping of an in vivo N-glycoproteome reveals rigid topological and sequence constraints. Cell **141:**897–907. http://dx.doi.org/10.1016/j.cell.2010.04.012.
47. **Zielinska DF, Gnad F, Schropp K, Wisniewski JR, Mann M.** 2012. Mapping N-glycosylation sites across seven evolutionarily distant species reveals a divergent substrate proteome despite a common core machinery. Mol Cell **46:**542–548. http://dx.doi.org/10.1016/j.molcel.2012.04.031.
48. **Valliere-Douglass JF, Eakin CM, Wallace A, Ketchem RR, Wang W, Treuheit MJ, Balland A.** 2010. Glutamine-linked and non-consensus asparagine-linked oligosaccharides present in human recombinant antibodies define novel protein glycosylation motifs. J Biol Chem **285:**16012–16022. http://dx.doi.org/10.1074/jbc.M109.096412.
49. **Sanderson CM, Frischknecht F, Way M, Hollinshead M, Smith GL.** 1998. Roles of vaccinia virus EEV-specific proteins in intracellular actin tail formation and low pH-induced cell-cell fusion. J Gen Virol **79:**1415–1425.
50. **Payne LG, Norrby E.** 1976. Presence of haemagglutinin in the envelope of extracellular vaccinia virus particles. J Gen Virol **32:**63–72. http://dx.doi.org/10.1099/0022-1317-32-1-63.
51. **Shida H.** 1986. Nucleotide sequence of the vaccinia virus hemagglutinin gene. Virology **150:**451–462. http://dx.doi.org/10.1016/0042-6822(86)90309-0.
52. **Zhang WH, Wilcock D, Smith GL.** 2000. Vaccinia virus F12L protein is required for actin tail formation, normal plaque size, and virulence. J Virol **74:**11654–11662. http://dx.doi.org/10.1128/JVI.74.24.11654-11662.2000.
53. **Parkinson JE, Smith GL.** 1994. Vaccinia virus gene A36R encodes a M(r) 43-50 K protein on the surface of extracellular enveloped virus. Virology **204:**376–390. http://dx.doi.org/10.1006/viro.1994.1542.
54. **Turner PC, Moyer RW.** 2006. The cowpox virus fusion regulator proteins SPI-3 and hemagglutinin interact in infected and uninfected cells. Virology **347:**88–99. http://dx.doi.org/10.1016/j.virol.2005.11.012.
55. **Payne LG.** 1979. Identification of the vaccinia hemagglutinin polypeptide from a cell system yielding large amounts of extracellular enveloped virus. J Virol **31:**147–155.
56. **McIntosh AA, Smith GL.** 1996. Vaccinia virus glycoprotein A34R is required for infectivity of extracellular enveloped virus. J Virol **70:**272–281.
57. **Bisht H, Weisberg AS, Szajner P, Moss B.** 2009. Assembly and disassembly of the capsid-like external scaffold of immature virions during vaccinia virus morphogenesis. J Virol **83:**9140–9150. http://dx.doi.org/10.1128/JVI.00875-09.
58. **Pompella A, Visvikis A, Paolicchi A, De Tata V, Casini AF.** 2003. The changing faces of glutathione, a cellular protagonist. Biochem Pharmacol **66:**1499–1503. http://dx.doi.org/10.1016/S0006-2952(03)00504-5.
59. **Pompella A, Corti A.** 2015. Editorial: the changing faces of glutathione, a cellular protagonist. Front Pharmacol **6:**98. http://dx.doi.org/10.3389/fphar.2015.00098.
60. **Fernandes AP, Holmgren A.** 2004. Glutaredoxins: glutathione-dependent redox enzymes with functions far beyond a simple thioredoxin backup system. Antioxid Redox Signal **6:**63–74. http://dx.doi.org/10.1089/152308604771978354.
61. **White CL, Senkevich TG, Moss B.** 2002. Vaccinia virus G4L glutaredoxin is an essential intermediate of a cytoplasmic disulfide bond pathway required for virion assembly. J Virol **76:**467–472. http://dx.doi.org/10.1128/JVI.76.2.467-472.2002.
62. **White CL, Weisberg AS, Moss B.** 2000. A glutaredoxin, encoded by the G4L gene of vaccinia virus, is essential for virion morphogenesis. J Virol **74:**9175–9183. http://dx.doi.org/10.1128/JVI.74.19.9175-9183.2000.
63. **Senkevich TG, White CL, Koonin EV, Moss B.** 2002. Complete pathway for protein disulfide bond formation encoded by poxviruses. Proc Natl Acad Sci U S A **99:**6667–6672. http://dx.doi.org/10.1073/pnas.062163799.
64. **Senkevich TG, Weisberg AS, Moss B.** 2000. Vaccinia virus E10R protein is associated with the membranes of intracellular mature virions and has a

role in morphogenesis. Virology **278:**244–252. http://dx.doi.org/10.1006/viro.2000.0656.

65. **Senkevich T, White C, Weisberg A, Granek J, Wolffe E, Koonin E, Moss B.** 2002. Expression of the vaccinia virus A2.5L redox protein is required for virion morphogenesis. Virology **300:**296–303. http://dx.doi.org/10.1006/viro.2002.1608.
66. **Eser M, Masip L, Kadokura H, Georgiou G, Beckwith J.** 2009. Disulfide bond formation by exported glutaredoxin indicates glutathione's presence in the E. coli periplasm. Proc Natl Acad Sci U S A **106:**1572–1577. http://dx.doi.org/10.1073/pnas.0812596106.
67. **Su HP, Garman SC, Allison TJ, Fogg C, Moss B, Garboczi DN.** 2005. The 1.51-angstrom structure of the poxvirus L1 protein, a target of potent neutralizing antibodies. Proc Natl Acad Sci U S A **102:**4240–4245. http://dx.doi.org/10.1073/pnas.0501103102.
68. **Blouch RE, Byrd CM, Hruby DE.** 2005. Importance of disulphide bonds for vaccinia virus L1R protein function. Virol J **2:**91. http://dx.doi.org/10.1186/1743-422X-2-91.
69. **Mohorko E, Glockshuber R, Aebi M.** 2011. Oligosaccharyltransferase: the central enzyme of N-linked protein glycosylation. J Inherit Metab Dis **34:**869–878. http://dx.doi.org/10.1007/s10545-011-9337-1.
70. **Maruri-Avidal L, Weisberg AS, Moss B.** 2013. Association of the vaccinia virus A11 protein with the endoplasmic reticulum and crescent precursors of immature virions. J Virol **87:**10195–10206. http://dx.doi.org/10.1128/JVI.01601-13.
71. **Maruri-Avidal L, Weisberg AS, Moss B.** 2013. Direct formation of vaccinia virus membranes from the endoplasmic reticulum in the absence of the newly characterized L2-interacting protein A30.5. J Virol **87:**12313–12326. http://dx.doi.org/10.1128/JVI.02137-13.